Journal of Autoimmunity 41 (2013) 6–16

Contents lists available at SciVerse ScienceDirect

Journal of Autoimmunity

journal homepage: www.elsevier.com/locate/jautimm

Identification of novel markers in rheumatoid arthritis through integrated analysis of DNA methylation and microRNA expression

Lorenzo de la Rica [a], José M. Urquiza [a], David Gómez-Cabrero [b], Abul B.M.M.K. Islam [c,d], Nuria López-Bigas [c,e], Jesper Tegnér [b], René E.M. Toes [f], Esteban Ballestar [a,*]

[a] Chromatin and Disease Group, Cancer Epigenetics and Biology Programme (PEBC), Bellvitge Biomedical Research Institute (IDIBELL), 08907 L'Hospitalet de Llobregat, Barcelona, Spain
[b] Department of Medicine, Karolinska Institutet, Computational Medicine Unit, Centre for Molecular Medicine, Swedish e-science Research Centre (SeRC), Solna, Stockholm, Sweden
[c] Department of Experimental and Health Sciences, Barcelona Biomedical Research Park, Universitat Pompeu Fabra (UPF), 08003 Barcelona, Spain
[d] Department of Genetic Engineering and Biotechnology, University of Dhaka, Dhaka 1000, Bangladesh
[e] Institució Catalana de Recerca i Estudis Avançats (ICREA), Barcelona, Spain
[f] Department of Rheumatology, Leiden University Medical Center, Leiden, The Netherlands

ARTICLE INFO

Article history:
Received 14 December 2012
Accepted 16 December 2012

Keywords:
Rheumatoid arthritis
Rheumatoid arthritis synovial fibroblasts
DNA methylation
Epigenetic
MicroRNAs
Integration

ABSTRACT

Autoimmune rheumatic diseases are complex disorders, whose etiopathology is attributed to a crosstalk between genetic predisposition and environmental factors. Both variants of autoimmune susceptibility genes and environment are involved in the generation of aberrant epigenetic profiles in a cell-specific manner, which ultimately result in dysregulation of expression. Furthermore, changes in miRNA expression profiles also cause gene dysregulation associated with aberrant phenotypes. In rheumatoid arthritis, several cell types are involved in the destruction of the joints, synovial fibroblasts being among the most important. In this study we performed DNA methylation and miRNA expression screening of a set of rheumatoid arthritis synovial fibroblasts and compared the results with those obtained from osteoarthritis patients with a normal phenotype. DNA methylation screening allowed us to identify changes in novel key target genes like *IL6R*, *CAPN8* and *DPP4*, as well as several *HOX* genes. A significant proportion of genes undergoing DNA methylation changes were inversely correlated with expression. miRNA screening revealed the existence of subsets of miRNAs that underwent changes in expression. Integrated analysis highlighted sets of miRNAs that are controlled by DNA methylation, and genes that are regulated by DNA methylation and are targeted by miRNAs with a potential use as clinical markers. Our study enabled the identification of novel dysregulated targets in rheumatoid arthritis synovial fibroblasts and generated a new workflow for the integrated analysis of miRNA and epigenetic control.

1. Introduction

Rheumatoid arthritis (RA) is a chronic autoimmune inflammatory disease characterized by the progressive destruction of the joints. RA pathogenesis involves a variety of cell types, including several lymphocyte subsets, dendritic cells, osteoclasts and synovial fibroblasts (SFs). In healthy individuals, SFs are essential to keep the joints in shape, doing so by providing nutrients, facilitating matrix remodeling and contributing to tissue repair [1]. In contrast to normal SFs or those isolated from patients with osteoarthritis (osteoarthritis synovial fibroblasts, OASFs), rheumatoid arthritis synovial fibroblasts (RASFs) show activities associated with an aggressive phenotype, like upregulated expression of protooncogenes, specific matrix-degrading enzymes, adhesion molecules, and cytokines [2]. Differences in phenotype and gene expression between RASFs and their normal counterparts reflect a profound change in processes involved in gene regulation at the transcriptional and post-transcriptional levels. The first group comprises epigenetic mechanisms, like DNA methylation, whilst miRNA control constitutes one of the best studied mechanisms of the second.

DNA methylation takes place in cytosine bases followed by guanines. In relation with transcription, the repressive role of methylation at CpG sites located at or near the transcription start sites of genes, especially when those CpGs are clustered as CpG islands, is well established [3]. Methylation of CpGs located in other

* Corresponding author. Tel.: +34 932607133; fax: +34 932607219.
E-mail address: eballestar@idibell.org (E. Ballestar).

0896-8411/$ – see front matter © 2012 Elsevier Ltd. All rights reserved.
http://dx.doi.org/10.1016/j.jaut.2012.12.005

regions like gene bodies is also involved in gene regulation [4,5]. At the other side of gene regulation lie microRNAs (miRNAs), a class of endogenous, small, non-coding regulatory RNA molecules that modulate the expression of multiple target genes at the post-transcriptional level and that are implicated in a wide variety of cellular processes and disease pathogenesis [6].

The study of epigenetic- and miRNA-mediated alterations in association with disease is becoming increasingly important as these processes directly participate in the generation of aberrant profiles of gene expression ultimately determining cell function and are pharmacologically reversible. Epigenetics is particularly relevant in autoimmune rheumatic diseases as it is highly dependent on environmental effects. As indicated above, both genetics and environmental factors contribute to ethiopathology of autoimmune rheumatic disorders. This double contribution is typically exemplified by the partial concordance in monozygotic twins (MZ) [7,8]. It is of inherent interest to identify autoimmune disease phenotypes for which the environment plays a critical role [9]. Many environmental factors, including exposure to chemicals, tobacco smoke, radiation, ultraviolet (UV) light and infectious agents among other external factors, are associated with the development of autoimmune rheumatic disorders [10]. Most of these environmental factors are now known to directly or indirectly induce epigenetic changes, which modulate gene expression and therefore associate with changes in cell function. For this reason, epigenetics provides a source of molecular mechanisms that can explain the environmental effects on the development of autoimmune disorders [11]. The close relationship between environment and epigenetic status and autoimmune rheumatic disease is also exemplified by using animal models [12]. This type of studies is also essential for the identification of novel clinical markers for disease onset, progression and response to treatments.

In this line, initial reports demonstrated hypomethylation-associated reactivation of endogenous retroviral element L1 in the RA synovial lining at joints [13]. Additional sequences have since been found to undergo hypomethylation in RASFs, like *IL-6* [14] and *CXCL12* [15]. Candidate gene analysis has also enabled genes to be identified that are hypermethylated in RASFs [16]. More recently, DNA methylation profiling of RASFs versus OASFs has led to the identification of a number of hypomethylated and hypermethylated genes [17]. With respect to miRNAs, reduced miR-34a levels have been linked with increased resistance of RASFs to apoptosis [18], and lower miR-124a levels in RASFs impact its targets, CDK-2 and MCP-1 [19]. Conversely, miR-203 shows increased expression in RASFs [20]. Interestingly, overexpression of this miR-203 is demethylation-dependent, highlighting the importance of investigating multiple levels of regulation and the need to use integrated strategies that consider interconnected mechanisms.

In this study, we have performed the first integrated comparison of DNA methylation and miRNA expression data, together with mRNA expression data from RASFs versus OASFs (Fig. 1) in order to investigate the relevance of these changes in these cells and to overcome the limitations of using a small number of samples. Our analysis identifies novel targets of DNA methylation- and miRNA-associated dysregulation in RA. Integration of the analysis of these two datasets suggests the existence of several genes for which the two mechanisms could act in the same or in opposite directions.

2. Material and methods

2.1. Subjects and sample preparation

Fibroblast-like synoviocytes (FLSs) were isolated from synovial tissues extracted from RA and OA patients at the time of joint replacement in the Department of Rheumatology of Leiden University Medical Center. All RA patients met the 1987 criteria of the American College of Rheumatology. Before tissue collection, permission consistent with the protocol of the Helsinki International Conference on Harmonisation Good Clinical Practice was obtained. All individuals gave informed consent. Synovial tissues

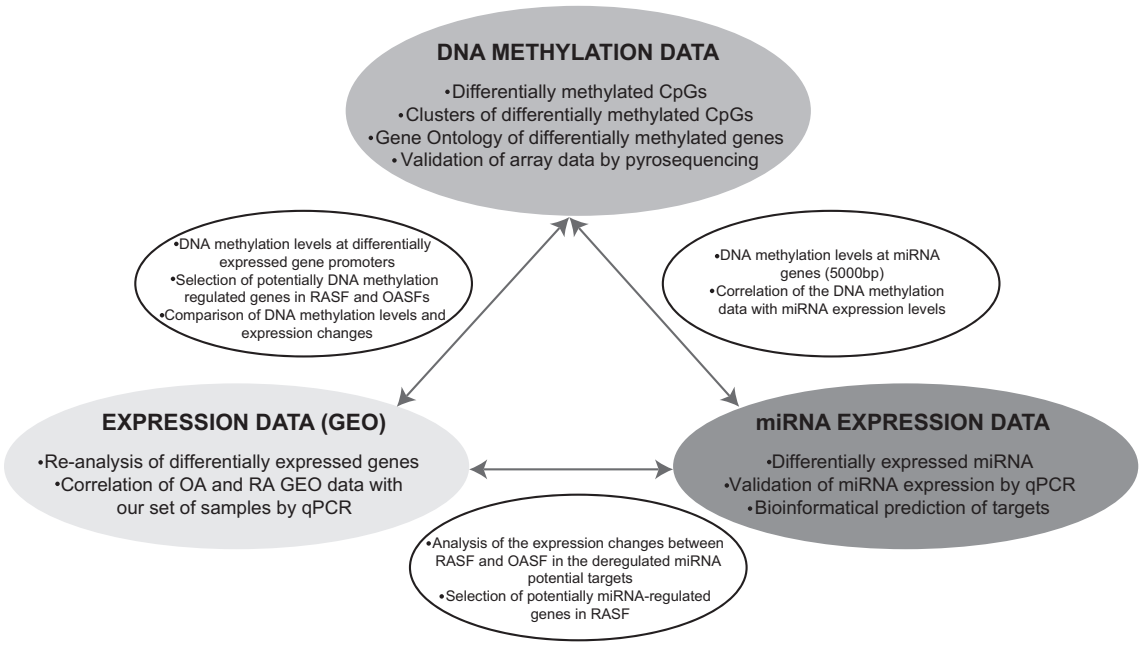

Fig. 1. Scheme depicting the strategy designed in this study where DNA methylation and miRNA data are integrated with expression array data. The grey oval areas show the type of information that individual analysis of DNA methylation, miRNA expression and expression datasets can provide. This is listed within these grey oval areas and are described in detail in the Results section. Between these grey oval areas, smaller elliptical panels show the type of analysis that can provide the combined information between DNA methylation and expression datasets (left), DNA methylation and miRNA expression datasets (right), or expression and miRNA expression datasets (bottom).

were collected during the arthroscopy, frozen in Tissue-Tek OCT compound (Sakura Finetek, Zoeterwoude, Netherlands) and cut into 5-μm slices using a cryotome (Leica CM 1900). Fibroblast cultures were maintained in Dulbecco's modified Eagle's medium supplemented with 10% fetal calf serum.

2.2. DNA methylation profiling using universal bead arrays

Infinium HumanMethylation450 BeadChips (Illumina, Inc.) were used to analyze DNA methylation. With this analysis it is possible to cover >485,000 methylation sites per sample at single-nucleotide resolution. This panel covers 99% of RefSeq genes, with an average of 17 CpG sites per gene region distributed across the promoter, 5′UTR, first exon, gene body, and 3′UTR. It covers 96% of CpG islands, with additional coverage in island shores and the regions flanking them. Bisulfite conversion of DNA samples was done using the EZ DNA methylation kit (Zymo Research, Orange, CA). After bisulfite treatment, the remaining assay steps were identical to those of the Infinium Methylation Assay, using reagents and conditions supplied and recommended by the manufacturer. Two technical replicates of each bisulfite-converted sample were run. The results were all in close agreement and were averaged for subsequent analysis. The array hybridization was conducted under a temperature gradient program, and arrays were imaged using a BeadArray Reader (Illumina Inc.). The image processing and intensity data extraction software and procedures were those described by Bibikova and colleagues [21]. Each methylation datum point was represented as a combination of the Cy3 and Cy5 fluorescent intensities from the M (methylated) and U (unmethylated) alleles. Background intensity, computed from a set of negative controls, was subtracted from each datum point.

2.3. Detection of differentially methylated CpGs

Differentially methylated CpGs were selected using an algorithm in the statistical computing language R [22], version 2.14.0. In order to process Illumina Infinium HumanMethylation450 methylation data, we used the methods available in the LIMMA and LUMI packages [23] from the Bioconductor repository [24]. Before statistical analysis, a pre-process stage was applied, whose main steps were: 1) Adjusting color balance, i.e., normalizing between two color channels; 2) Quantile normalizing based on color balance-adjusted data; 3) Removing probes with a detection p-value > 0.01; 4) Filtering probes located in sex chromosomes; 5) Filtering probes considered to be SNPs (single nucleotide polymorphisms). Specifically, the probes were filtered out using Illumina identifiers for SNPs, i.e. those probes with an "rs" prefix in their name; 6) Non-specific filtering based on the IQR (interquartile range) [25], using 0.20 as the threshold value.

Subsequently, a Bayes-moderated t-test was carried out using LIMMA [26]. Several criteria have been proposed to identify significant differences in methylated CpGs. In this study, we adopted the median-difference beta-value between the two sample groups for each CpG [27,28]. Specifically we considered a probe as differentially methylated if (1) the absolute value of the median-difference between b-values is higher than 0.1 and the statistical test was significant (p-value < 0.05).

2.4. Identification of genomic clusters of differentially methylated CpGs

A clustering method available in Charm package [29] was applied to the differentially methylated CpGs. Although Charm is a package specific for analyzing DNA methylation data from two-color Nimblegen microarrays, we reimplemented the code to invoke the main clustering function using genomic CpG localization. By using this approach, we identified Differentially Methylated Regions (DMR) by grouping differentially methylated probes closer than 500 pbs. In this analysis, the considered lists of CpGs were those associated with a value of $p < 0.01$.

2.5. Bisulfite pyrosequencing

CpGs were selected for technical validation of Infinium Methylation 450K by the bisulfite pyrosequencing technique in the RASF and OASF samples. CpG island DNA methylation status was determined by sequencing bisulfite-modified genomic DNA. Bisulfite modification of genomic DNA was carried out as described by Herman and colleagues [30]. 2 μl of the converted DNA (corresponding to approximately 20–30 ng) were then used as a template in each subsequent PCR. Primers for PCR amplification and sequencing were designed with the PyroMark® Assay Design 2.0 software (Qiagen). PCRs were performed with the HotStart Taq DNA polymerase PCR kit (Qiagen) and the success of amplification was assessed by agarose gel electrophoresis. Pyrosequencing of the PCR products was performed with the Pyromark™ Q24 system (Qiagen). All primer sequences are listed in Supplementary Table 1.

2.6. Gene expression data analysis and comparison of DNA expression and DNA methylation data

To compare expression and methylation data, we used RASF and OASF expression data from the Gene Expression Omnibus (GEO) under the accession number (GSE29746) [31]. Agilent one-color expression data were examined using LIMMA [24]. The pre-process stage consisted of background correction, followed by normalization. Thus, the applied background correction is a convolution of normal and exponential distributions that are fitted to the foreground intensities using the background intensities as a covariate, as explained in the LIMMA manual. Next, a well-known quantile method was performed to normalize the green channel between the arrays and then the green channel intensity values were log2-transformed. Values of average replicate spots were analyzed with a Bayes-moderated t-test. Expression genes matching methylated genes were then studied. Genes differentially expressed between RASF and OASF groups were selected if they met the criteria of having values of p and FDR (False Discovery Rate) lower than 0.05 as calculated by Benjamini-Hochberg and a greater than two-fold or less than 0.5-fold change in expression. Expression data were validated by quantitative RT-PCR. Primer sequences are listed in Supplementary Table 1.

2.7. microRNA expression screening, target prediction and integration with DNA methylation data

Total RNA was extracted with TriPure (Roche, Switzerland) following the manufacturer's instructions. Ready-to-use microRNA PCR Human Panel I and II V2.R from Exiqon (Reference 203608) were used according to the instruction manual (Exiqon). For each RT-PCR reaction 30 ng of total RNA was used. Samples from OASF and RASF patients were pooled and two replicates of each group were analyzed on a Roche LightCycler® 480 real-time PCR system. Results were converted to relative values using the inter-plate calibrators included in the panels (log 2 ratios). RASF and OASF average expression values were normalized with respect to reference gene miR-103. Differentially expressed microRNAs (FC > 2 or < 0.5) were selected.

To predict the potential targets of the dysregulated microRNAs, we used the algorithms of several databases, specifically TargetScan

[32], PicTar [33], PITA [34], miRBase [35], microRNA.org [36], miRDB/MirTarget2 [37], TarBase [38], and miRecords [39], StarBase/CLIPseq [40]. Only targets predicted in at least four of these databases and differentially expressed between RASFs and OASFs were included in the heatmaps.

To compare the DNA methylation bead array data with the miRNA expression levels, miRNAs were mapped to Illumina 450k probes. For each differentially expressed miRNA we studied the CpGs within a 5000 bp window around the transcription start site. Using the GRCh37 assembly annotation for Illumina, the genomic localization of probes was extracted in order to match them with miRNA loci. Genomic features of miRNAs were taken from the miRBase [41] and Illumina annotation was obtained from IlluminaHumanMethylation450K.db Bioconductor Package [41].

2.8. Gene ontology analysis

Gene Ontology analysis was done with the FatiGO tool [42], which uses Fisher's exact test to detect significant over-representation of GO terms in one of the sets (list of selected genes) with respect to the other one (the rest of the genome). Multiple test correction to account for the multiple hypothesis tested (one for each GO term) is applied to reduce false positives. GO terms with adjusted P-value < 0.05 are considered significant.

2.9. Graphics and heatmaps

All graphs were created using Prism5 Graphpad. Heatmaps were generated from the expression or methylation data using the Genesis program from Graz University of Technology [43].

3. Results

3.1. Comparison of DNA methylation patterns between RASF and OASF reveals both hypomethylation and hypermethylation of key genes

We performed high-throughput DNA methylation screening to compare SF samples from six RA and six OA patients. To this end, we used a methylation bead array that allows the interrogation of >450,000 CpG sites across the entire genome covering 99% of RefSeq genes. Statistical analysis of the combined data from the 12 samples showed that 2571 CpG sites, associated with 1240 different genes, had significant differences in DNA methylation between RASFs and OASFs (median β differences > 0.10, $p < 0.05$) (Fig. 2A and Supplementary Table 2). Specifically, we found 1091 hypomethylated CpG sites (in 575 genes) and 1479 hypermethylated CpG sites (in 714 genes).

The list of genes differentially methylated between RASFs and OASFs includes a number with known implications for RA pathogenesis and some potentially interesting novel genes (Table 1). One of the best examples is *IL6R*. Our results indicated that *IL6R* is hypomethylated in RASFs with respect to OASFs, and that hypomethylation is probably associated with *IL6R* overexpression in RASFs. *IL6* and *IL6R* are factors well known to be associated with RA pathogenesis and progression. *IL6R* overexpression plays a key role in acute and chronic inflammation and increases the risk of joint destruction in RA. Also, IL6R antibodies have recently been approved for the treatment of RA [44]. Another interesting example in the hypomethylated gene list is *TNFAIP8*, or *TIPE2*, a negative mediator of apoptosis that plays a role in inflammation [45]. We also identified *CAPN8* as the gene with the greatest difference between RASFs and OASFs. This gene has not previously been associated with RA, although it is involved in other inflammatory processes such as irritable bowel syndrome [46]. Conversely, hypermethylated genes include factors like *DPP4* and *CCR6*. *DPP4* encodes a serine protease, which cleaves a number of regulatory factors, including chemokines and growth factors. DPP4 inhibitors have recently emerged as novel pharmacological agents for inflammatory disease [47]. Several lines of evidence have also shown a role for *CCR6* in RA [48].

We then set out to determine whether our differentially methylated genes could be involved in biological functions relevant to RA pathogenesis. We therefore performed Gene Ontology analysis to test whether some molecular functions or biological processes were significantly associated with the genes with the greatest difference in DNA methylation status between RASFs and OASFs. The analysis was performed independently for gene lists in the hypomethylated and hypermethylated group. We observed significantly enriched functional processes that are potentially relevant in the biology of SFs (Fig. 2B), including the following categories: focal adhesion assembly (GO:0048041), cartilage development (GO:0051216) and regulation of cell growth (GO:0001558) for hypomethylated genes. For hypermethylated genes, we observed enrichment in categories such as response to wounding (GO:0009611), cell migration (GO:0016477) and cell adhesion (GO:0007155). Hypermethylated and hypomethylated genes shared several functional categories, such as cell differentiation (GO:0030154), cell adhesion (GO:0007155) and skeletal system development (GO:0001501) characteristic of this cell type.

We also compared our data with those reported in a recent study by Nakano and colleagues [17]. We found a significant overlap of genes that were hypomethylated and hypermethylated in both sets of samples (Supp. Fig. 1). These included genes like *MMP20*, *RASGRF2* and *TRAF2* from the list of hypomethylated genes, and *ADAMTS2*, *EGF* and *TIMP2* from among the hypermethylated genes (see Supp. Fig. 1 and Table 2 in [17]). The use of a limited set of samples in the identification of genes introduces a bias associated with each particular sample cohort, which would explain the partial overlap between different experiments. However in this case, we observed an excellent overlap between both experiments.

We also performed an analysis to identify genomic clusters of differentially methylated CpGs, which highlighted several regions of consecutive CpGs that are hypomethylated or hypermethylated in RASFs compared with OASFs. Among hypermethylated CpG clusters in RASFs we identified *TMEM51* and *PTPRN2*. With respect to hypomethylated genes, up to nine clustered CpGs were hypomethylated around the transcription start sites of *HOXA11* (Fig. 2C, left) and nine in *CD74*, the major histocompatibility complex, class II invariant chain-encoding gene. CD74 levels have been reported to be higher in synovial tissue samples from patients with RA than in tissue from patients with osteoarthritis [49]. *HOXA11* was considered another interesting gene, as HOX genes are a direct target of EZH2, a Polycomb group protein involved in differentiation and in establishing repressive marks, including histone H3K27me3 and DNA methylation, under normal and pathological conditions. In fact, additional HOXA genes were identified as being differentially methylated between RASFs and OASFs (Table 1), suggesting that the Polycomb group differentiation pathway may be responsible for these differences.

To validate our analysis, we used bisulfite pyrosequencing of selected genes (Supp. Fig. 2). In all cases, pyrosequencing of individual genes confirmed the results of the analysis. In fact, comparison of the bead array and pyrosequencing methylation data (Fig. 2C, center and right) showed an excellent correlation, supporting the validity of our analysis. Additional genes that were subjected to pyrosequencing analysis included *CAPN8* and *IL6R*, both of which were hypomethylated in RASFs, and *DPP4* and *HOXC4*

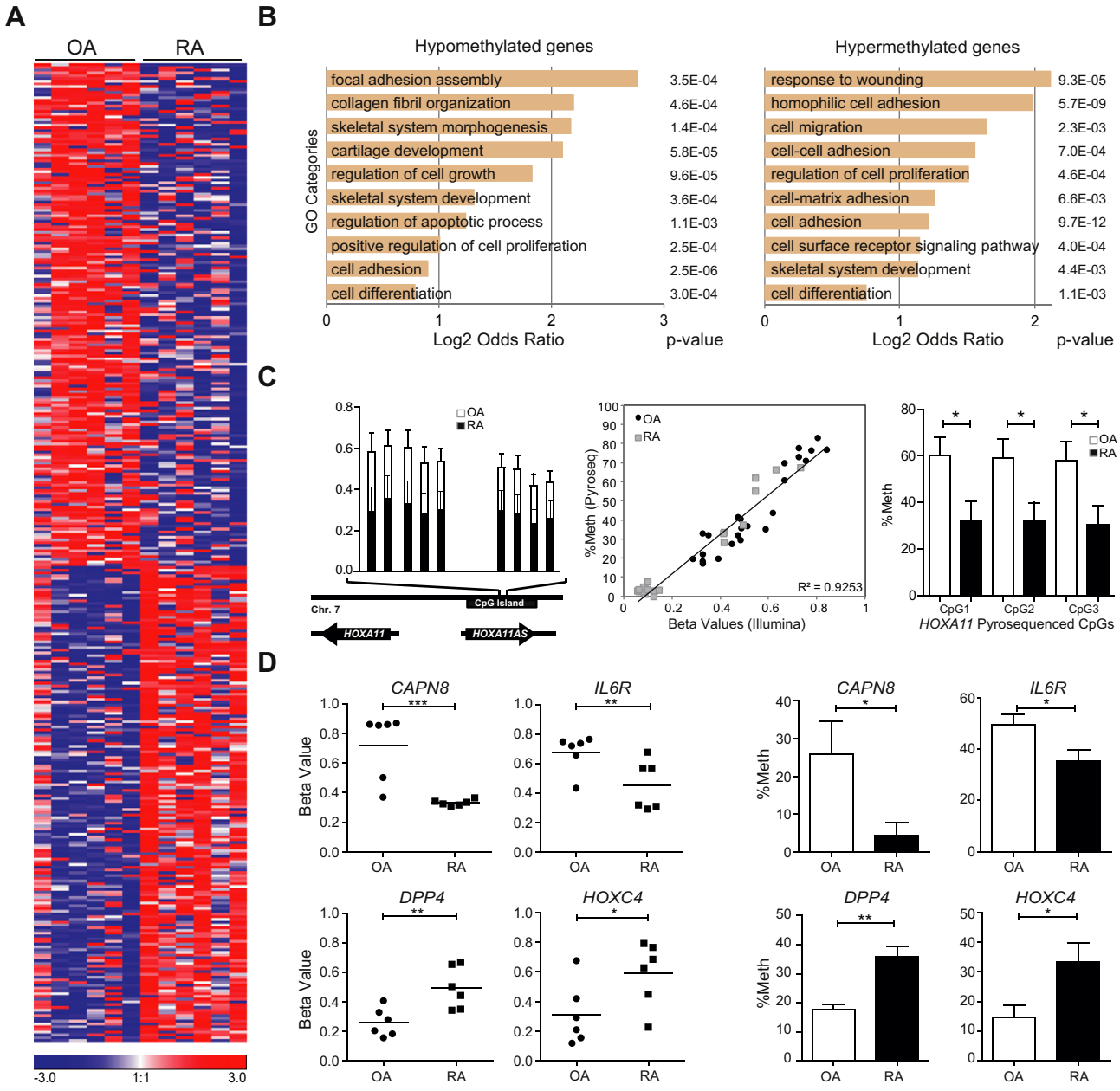

Fig. 2. Comparison of the DNA methylation profiles between RASFs and OASFs samples. (A) Heatmap including the methylation data for the six RASF and OASF samples shows significant differential methylation. There are both significant hypermethylated and hypomethylated genes. In this heatmap, all the genes with a value of $p < 0.05$ and a difference in median $\beta > 0.2$ are shown. The scale at the bottom distinguishes hypermethylated (red) and hypomethylated (blue) genes. (B) Summary of the gene ontology (GO) analysis for the category "biological process" among hypomethylated and hypermethylated genes. *P*-values are shown on the right (C) Methylation data from the array analysis corresponding to HOXA11 gene in which 9 consecutive CpGs are hypomethylated in RASFs relative to OASFs (left), comparison of the array data and pyrosequencing, where the excellent correlation between the two sources of data is shown by a regression line (center), methylation values as obtained through pyrosequencing corresponding to three selected CpGs comparing RASF and OASF samples. (D) Comparison of the array data (left) and pyrosequencing data (right) of four selected hypomethylated (*CAPN8*, *IL6R*) and hypermethylated (*DPP4*, *HOXC4*) genes.

in the hypermethylated group (Fig. 2D and E). In all cases, the analysis was validated by pyrosequencing in a larger cohort of samples.

3.2. Integration of DNA methylation data with expression data from RASFs and OASFs

DNA methylation is generally associated with gene repression, particularly when it occurs at promoter CpG islands. However, DNA methylation changes at promoters with low CpG density can also regulate transcription, and changes in gene bodies also affect transcriptional activity [4], although they do not necessarily repress it. We therefore integrated our DNA methylation data with a high-throughput expression analysis of RASFs and OASFs from a recent study (GSE29746) [31]. To integrate expression data with our methylation results, we first reanalyzed the expression data as described in the Materials and Methods. Applying the threshold criterion of a value of $p < 0.01$, we identified 3470 probes differentially expressed between RASFs and OASFs (for which FC > 2 or <0.6) (Fig. 3A). We then compared the results from the analysis of the expression arrays with the DNA methylation data. Our analysis showed that 208 annotated CpGs displayed an inverse correlation between expression and methylation levels (Fig. 3B and Supplementary Table 3).

Table 1
Selection of genes differentially methylated and/or expressed in RASF vs. OASF, and previously described implications in RA.

Gene name	Δmeth CpG	Region	Description	Δ beta (RA-OA)	FC express (RA/OA)	Previously reported RA implication (ref)
CAPN8	1	Body	Calpain 8	−0.52	N/A	
SERPINA5	1	TSS1500	Serpin peptidase inhibitor, clade A member 5	−0.40	N/A	
FCGBP	1	Body	Fc fragment of IgG binding protein	−0.35	0.34	Detected in plasma sera related with autoimmunity [56]
HOXA11	13	TSS1500	Homeobox A11	−0.30	0.40	
IL6R	1	Body	Interleukin 6 receptor	−0.29	N/A	Its ligand (IL6) is overexpressed in RA [57]
S100A14	3	TSS1500	S100 calcium binding protein A14	−0.27	N/A	Involved in invasion through MMP2 (elevated in RA plasma) [50]
TMEM51	2	5′UTR	Transmembrane protein 51	−0.27	4.21	
CSGALNACT1	3	TSS200	Chondroitin sulfate N-acetylgalactosaminyltransferase 1	−0.22	0.48	Involved in cartilage development and endocondral ossification [58] and [59]
COL14A1	2	Body	Collagen, type XIV, alpha 1	−0.22	3.76	
CD74	8	TSS1500	CD74 molecule	−0.22	N/A	Initiates MIF signal transduction (levels related with RA course) [60]
TNFAIP8	3	Body	Tumor necrosis factor, alpha-induced protein 8	−0.20	3.75	Negative regulator of innate and adaptative immunity [45]
TNFRSF8	1	Body|TSS 1500	Tumor necrosis factor receptor superfamily, member 8	−0.19	2.93	Its overexpression contributes to proinflammatory immune responses [61]
KCNJ15	2	5′UTR|TSS 200	Potassium inwardly-rectifying channel, subfamily J, member 15	−0.15	5.51	
CCR6	1	TSS1500	Chemokine (C-C motif) receptor 6	0.23	0.67	Migration, proliferation, and MMPs production [62]
DPP4	1	TSS200	Dipeptidyl-peptidase 4	0.23	N/A	Its inhibition increases cartilage invasion by RASF [63]
PRKCZ	17	Body|TSS 1500	Protein kinase C, zeta	0.25	N/A	Inactivates syndecan-4 (integrin co-receptor), reducing DC motility [64]
HLA-DRB5	3	Body	Major histocompatibility complex, class II, DR beta 5	0.26	3.16	SNP associated with cutaneous manifestations rheumatoid vasculitis [65]
ALOX5AP	1	TSS1500	Arachidonate 5-lipoxygenase-activating protein	0.29	N/A	Deficit of this molecule ameliorates symptoms in CIA [66]
BCL6	2	Body	B-cell CLL/lymphoma 6	0.30	N/A	RA synovial T cells express BCL6, potent B cell regulator [67]
SPTBN1	2	TSS1500	Spectrin, beta, non-erythrocytic 1	0.27	0.23	Associated with CD43 abrogates T cell activation [68]
HOXC4	13	5′UTR|TSS 1500	Homeobox C4	0.4	N/A	

To examine the relationship between methylation and gene expression further, we also performed an analysis focusing on the relative position of the CpG site that undergoes a significant change in methylation. We found that genes with a methylation change at the TSS or the 5′UTR generally exhibited an inverse correlation between DNA methylation and gene expression (Fig. 3C), whereby an increase in methylation tended to be accompanied by a decrease in expression. Curiously, this relationship is positive when looking at CpGs containing probes located at gene bodies with a significant methylation change (Fig. 3C). Fig. 3D shows two examples of an inverse correlation between DNA methylation and expression data.

We performed quantitative RT-PCR to investigate the expression status of several of the genes displaying a change in DNA methylation in the set of samples used in this study. This analysis included several of the genes mentioned above, as well as others, like *MMP2*, for which increased expression in RASFs has been described [50]. Our analysis confirmed the elevated levels for this gene in our collection of RASFs (Fig. 3E). We also observed an inverse correlation between DNA methylation and expression for genes like *HOXC4*, *HOXA11*, *CAPN8* and *IL6R* (Fig. 3F), although genes like *DPP4* did show a direct relationship. Specifically, we found that hypermethylated *DPP4* had higher levels of expression in RASFs than in OASFs (Fig. 3F). Elevated levels for *DPP4* are compatible with the data obtained by other researchers [51]. However, it also indicates that for some genes, other mechanisms contribute more to their expression levels than do DNA methylation changes.

3.3. *miRNA screening in RASF and OASF*

Changes in expression levels can certainly be due to transcriptional control, like that determined by epigenetic changes at gene promoters, DNA methylation, or differences in transcription factor binding. At the post-transcriptional level, miRNAs are recognized as being major players in gene expression regulation. We compared the expression levels of miRNAs in pooled RASF and OASF RNA samples. The screening led to the identification of a number of miRNAs that are overexpressed in RASFs with respect to OASFs, as well as downregulated miRNAs (Fig. 4A). Among the most upregulated and downregulated miRNAs, we identified several that have been previously associated with relevant or related events like miR-203 [20], which is upregulated in RASFs with respect to OASFs, and miR-124, which is downregulated in RASFs [52] (Fig. 4B). Other additional miRNAs identified in previous work in relation to RA include miR-146a and miR-34a (Fig. 4A). As indicated above, the overlap with other studies highlights the robustness of our data. However, it is likely that the analysis of a limited number of samples introduces a bias associated with specific characteristics of the samples in the studied cohort. Integrated analysis can help to identify relevant targets. We then performed quantitative PCR to validate a selection of the miRNAs in the entire cohort. Examples of miR-625*, downregulated in RASF, and miR-551b, upregulated in RASF, are shown in Fig. 4C.

As explained, miRNA-dependent control is associated with the expression control of a number of targets either by inducing direct mRNA degradation or through translational inhibition [53]. Accumulated evidence has shown that most miRNA targets are affected at the mRNA levels, and therefore comparison of mRNA expression array and

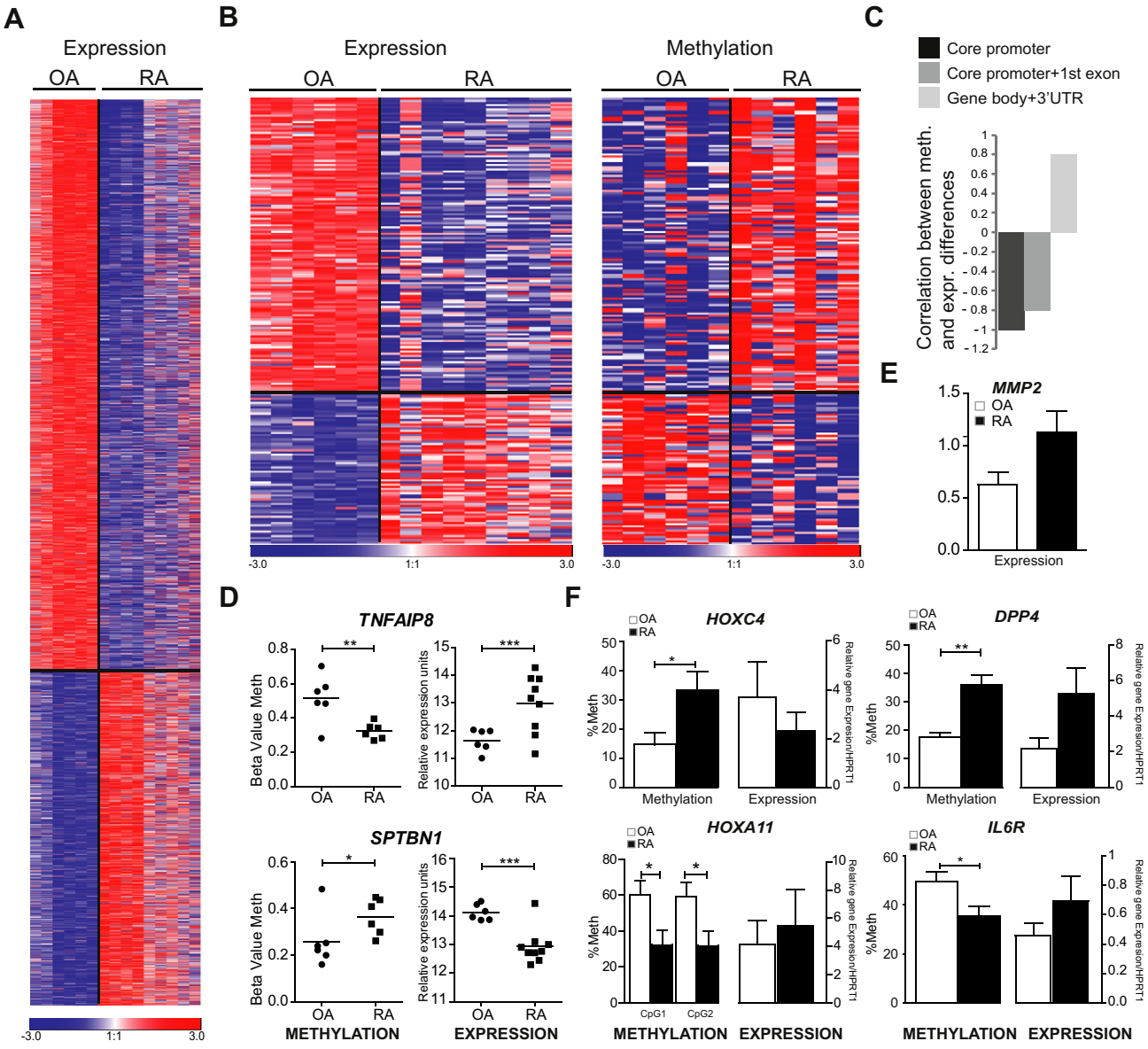

Fig. 3. Integration of DNA methylation with expression data. (A) Heatmaps including the reanalysis of expression data (GSE29746) for a collection of RASF and OASF samples. The scale at the bottom distinguishes upregulated (red) and downregulated (blue) genes. (B) Heatmap comparison of inversely correlated expression and methylation. (C) Correlation between differences in DNA methylation and expression of associated genes, focusing on different regions where the CpG sites are located in the probe, core promoter, core + 1st exon and gene body. (D) Illustrative examples of genes featuring an inverse correlation between methylation and expression. (E) Validation by quantitative RT-PCR of MMP2, previously described as overexpressed in RASFs. (F) Examples of genes whose expression data were validated by quantitative RT-PCR.

miRNA expression data is useful for identifying and evaluating the impact of miRNA misregulation at the mRNA levels.

To explore this aspect, we investigated the relationship between miRNA expression differences between RASFs and OASFs and their involvement in gene control by looking at levels of their potential targets. To this end, we obtained a matrix with the potential targets for each of the five miRNAs most strongly upregulated and downregulated in RASFs relative to OASFs. We considered *bona fide* putative targets those predicted by at least four databases. As before, we used the expression microarrays data for RASFs and OASFs generated in another study (GSE29746) [31].

When looking at the expression levels of putative targets of selected miRNAs we found more genes with potential effects on the RASF phenotype. These included genes like *CTSC*, *KLF8* or *EBF3*, which are upregulated in RASFs concomitant with downregulation of miR625* and *ITGBL1*, which is downregulated in RASF concomitant with upregulation of miR551b. Additional putative targets included TLR4 for miR-203 and NFAT5 for miR-124 (Fig. 4D). *TLR4* is upregulated in RA and plays a key role in the disease, whereas NFAT5 is a critical regulator of inflammatory arthritis.

3.4. Integrated analysis of both miRNAs and DNA methylation reveals multiple layers of regulation in genes relevant to RA pathogenesis

We performed two separate analyses to explore the potential connection between miRNA and DNA methylation control for genes associated with the RASF phenotype.

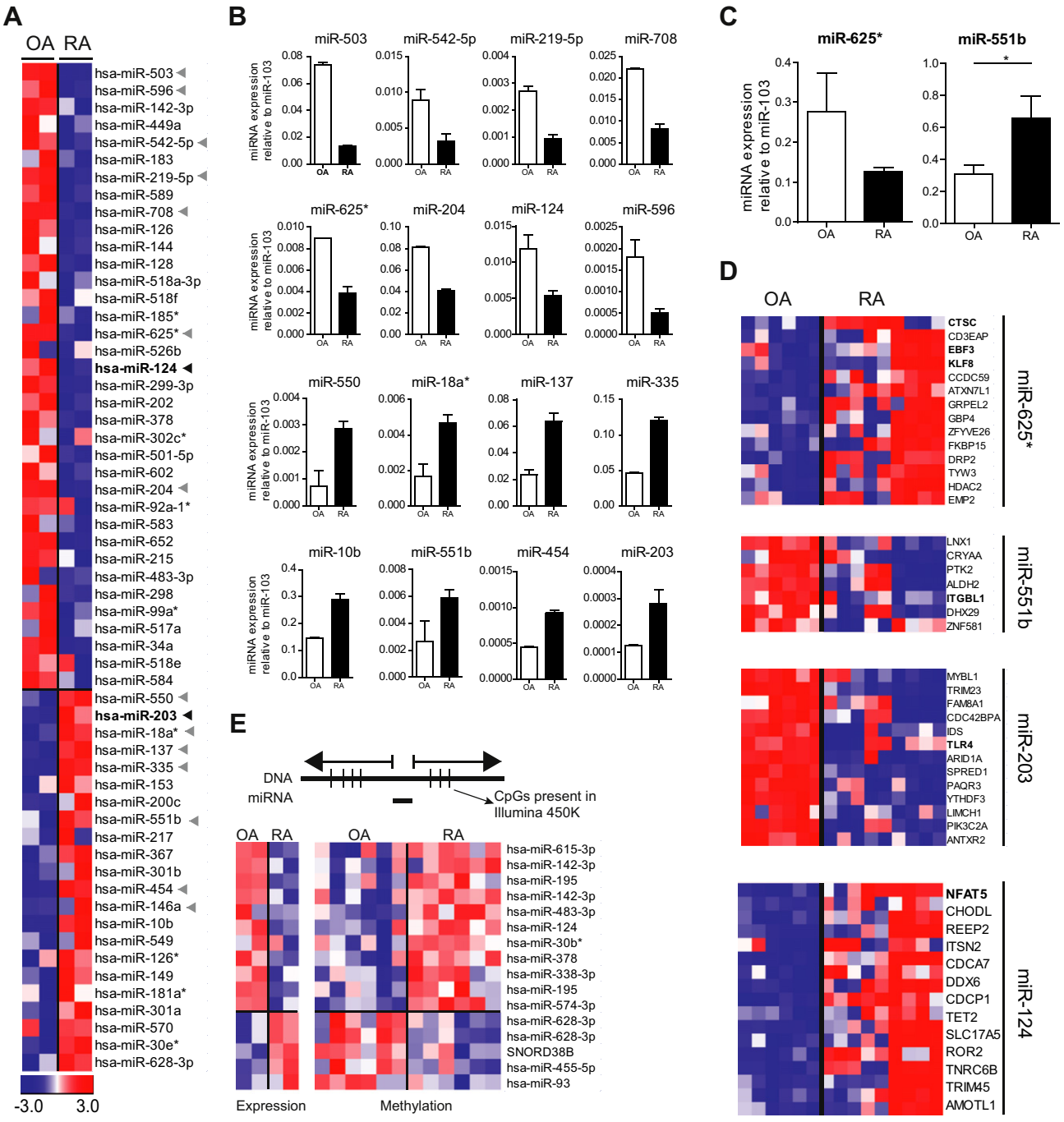

Fig. 4. miRNA dysregulation in RASF. (A) Heatmaps showing the miRNA expression data for pooled RASFs and OASFs. miRNAs previously described as dysregulated in RASFs are highlighted with a black arrow. Those represented in the adjacent section are highlighted with a grey arrow. The scale at the bottom distinguishes distinguishing upregulated (red) and downregulated (blue) genes. (B) Examples of the most upregulated and downregulated miRNAs in RASFs with respect to OASFs. (C) Validation of the miRNA data by quantitative RT-PCR. (D) Heatmaps showing the expression levels of putative targets (at least four hits for prediction in miRNA databases) for selected miRNAs in RASFs and OASFs. (E) Correlation between DNA methylation and miRNA expression data.

The first analysis focused on the potential regulation of miRNAs by DNA methylation. DNA methylation can also repress the expression of miRNAs, since miRNA-associated promoters are subjected to similar mechanisms of transcriptional control as protein-coding genes. We compared the data from the bead array analysis with miRNA expression data. Our analysis showed 11 downregulated miRNAs, like miR-124, that were located near CpG sites and were hypermethylated in RASFs. Only four upregulated miRNAs were located near a CpG site hypomethylated in RASFs (Fig. 4E).

The second analysis investigated the potential influence of DNA methylation and miRNA control on specific targets. As explained above, differences in expression patterns between RASFs and OASFs could be due to altered mechanisms of control at the epigenetic level, like DNA methylation, or at the post-transcriptional level. We generated a list of selected genes whose expression patterns differed significantly between RASFs and OASFs. Then we matched the expression data with our DNA methylation data from bead arrays and with a selection of miRNAs that might target those genes (as predicted at least by four databases) and that have significant

differences in expression between RASFs and OASFs. This yielded a list of genes potentially regulated by DNA methylation, at the transcriptional level, and targeted by miRNAs, at the post-transcriptional level. The list of genes comprises six groups (Supplementary Table 4): i) downregulated genes in which hypermethylation concurs with overexpression of a miRNA that targets them. Methylation and miRNA regulate in the same repressive direction in this group; ii) downregulated genes in which hypomethylation is potentially overcome by co-occurrence of upregulation of a miRNA that targets them. In this group, miRNA control is potentially the predominant mechanism; iii) downregulated genes in which hypermethylation predominates over downregulation of miRNAs that potentially target them; iv) upregulated genes in which hypomethylation concurs with downregulation of a miRNA that targets them; v) upregulated genes in which hypermethylation is overcome by downregulation of a miRNA that targets them, and, vi) upregulated genes in which hypermethylation predominates over upregulation of a miRNA that targets them. Integrated analysis would require further validation to provide *bona fide* targets determined by both regulatory mechanisms. However, this novel approach to integrating miRNA and DNA methylation analysis provides a new workflow for exploring the multiple layers of gene dysregulation in RA in greater depth.

4. Discussion

In this study we have identified novel dysregulated targets in rheumatoid arthritis (RA) synovial fibroblasts at the DNA methylation and miRNA expression levels. By using a double approach and integrated analysis of the DNA methylation, miRNA expression and mRNA expression data we have established a new pipeline for investigating the complexity of gene dysregulation in the context of this disease when using primary samples. As indicated above, dysregulation of gene expression arises from a combination of factors, including genetic polymorphisms in genes associated with regulatory roles and miRNAs, environmental factors and their combined effect on transcription factor function and epigenetic profiles, like DNA methylation and histone modification profiles. Understanding the relationship between different elements of regulation is key not only for understanding their intricate connections within the disease but also in the higher propensity to associated disorders [54]. DNA methylation-associated regulation and miRNA control are major regulatory elements and provide useful targets and markers of gene dysregulation in disease. In the context of RASFs, a few studies have previously shown the existence of genes with DNA methylation alterations in RASFs. Most of these have involved examining candidate genes. Examples include the identification of the *TNFRSF25* gene (encoding DDR9), which is hypermethylated at its CpG island in synovial cells of RA patients [16], and *CXCL12* upregulated and hypomethylated in RASFs [15]. More recently, Firestein and colleagues [17] took an array-based approach to identify hypomethylated and hypermethylated genes in RASFs. Regarding miRNA profiling in RASFs, several studies have demonstrated specific roles for miRNAs that are dysregulated in RA synovial tissues [18–20,55]. However, there were no previous systematic efforts to combine analyses of these two types of mechanisms in the context of RA.

To the best of our knowledge, our study constitutes the first attempt to integrate high-throughput omics data from primary samples in the context of RA. The need of integrating several levels of regulation is relevant for several reasons: first, from a biological point of view, it is essential to understand the molecular mechanisms underlying aberrant changes in gene expression associated with the acquisition of the aggressive phenotype of RASFs; second, from a more translational point of view, understanding multiple levels of regulation of target genes that undergo dysregulation in RA, could potentially allow to predict their behavior following the use of specific therapeutic compounds. It can also serve to make a better use of them as clinical markers of disease onset, progression or response to therapy.

Our analysis of individual datasets not only has allowed us to confirm changes described by others but also to determine novel genes with altered DNA methylation patterns, including *MMP20*, *RASGRF2*, *EGF*, *TIMP2* and others. Most importantly we have identified new genes that are relevant to the RA phenotype. This includes *IL6R*, which is well known as an overexpressed gene in RASFs and a target for antibody-based therapy [44]. Additional targets include *CAPN8*, *TNFAIP8*, *CD74* and *CCR6*. Methylation alterations in RASFs occur at promoter CpG islands in genes like *DPP4* or *HOXC4*, and downstream of the TSS in genes like *CAPN8* and *IL6R*. This last observation is in agreement with recent reports showing that gene expression can be also affected by methylation changes at gene bodies [4,5]. In any case, we have found a canonical inverse relationship between DNA methylation and expression status for a subset of more than 200 genes. At the miRNA level, analysis of the expression dataset has allowed us to validate previously described miRNAs, like miR-203 and miR-124, as well as identifying novel miRNAs, like miR-503, miR-625*, miR-551b, and miR-550, that are potentially associated with dysregulated targets in RASFs.

Integrative analysis has been carried out at different levels. Firstly, the combined analysis of DNA methylation and expression data generated a list of genes in which methylation changes were inversely correlated with expression changes. This list of genes potentially contains those regulated through DNA methylation in a canonical manner, where DNA methylation associates with gene repression (Supplementary Table 3). Secondly, we also studied the potential relationship between expression changes and miRNA expression changes that potentially target them (as defined by the cumulative use of miRNA target prediction databases). In this case, we identified a number of genes undergoing expression changes in RASFs that are potentially targeted by concomitantly dysregulated miRNAs.

Another level of integration is achieved by looking at genes that may be targeted or regulated by the combined action of miRNA and DNA methylation. Thus, we explored the potential combined effect of miRNAs and DNA methylation in genes undergoing expression changes in RASFs (Supplementary Table 2). Our analysis revealed gene targets in which methylation and miRNA control possibly concur in direction or have antagonistic effects. This classification of genes in different groups is important because pharmacological compounds or other experimental approaches influencing one of the mechanism (DNA methylation) but not the other (miRNA expression) or viceversa, would have to consider the existence of multiple levels of regulation for interpreting the outcome of such treatment. Finally, by looking at the potential control of miRNA expression by DNA methylation, we identified a further regulatory mechanism for several miRNAs, including miR-124. In this case, hypermethylation of a specific miRNA promoter, would have a positive effect on the expression levels of its targets, and, for instance, pharmacological demethylation of that miRNA would result in overexpression of the miRNA and downregulation of its targets.

As indicated above, epigenetic profiles and miRNA expression patterns are cell type-specific. The need to use primary samples for the target tissue or cell type of a particular disease is usually a limitation to performing epigenetic or miRNA analysis, given the access to small amounts of tissue or cells that can be obtained in most cases. The reduced number of laboratories with access to RASFs, OASFs or SF from normal individuals is a good reflection of

such limitation. Genetic analysis of genetically complex diseases does not have such a limitation, since in most cases can be done with peripheral blood. In this sense, the use of integrative approaches to investigate epigenetic and miRNA-mediated control of a limited set of samples overcomes partially this obstacle by providing extra sets of data for internal validation within a small cohort of samples and an increase of the robustness of the analysis.

In conclusion, our study highlights the need of investigating the multiple layers of regulation at the transcriptional and post-transcriptional levels as well as integrating the datasets during the analysis. As targets for therapy, it is important to understand the intricate connections between the various control mechanisms and to consider the existence of both processes that operate in the same direction or have antagonistic effects. The use of integrative approaches will also be necessary for the rational design of targeted therapies as well as for the use of different clinical markers for the classification. In this sense, the workflow designed in this study has allowed us to identify novel targets and their regulatory mechanism in RASF and opens up a number of possibilities for future research on epigenetics aspects on RA.

Acknowledgments

We would like to thank Dr. Gary Firestein for sharing the raw data of his DNA methylation study with us. We would also like to thank José Luis Pablos for his valuable feedback on his expression dataset. This work was supported by grant SAF2011-29635 from the Spanish Ministry of Science and Innovation, grant from Fundación Ramón Areces and grant 2009SGR184 from AGAUR (Catalan Government). LR is supported by a PFIS predoctoral fellowship and AI was supported by a AGAUR predoctoral fellowship. NL-B acknowledges funding from the Spanish Ministry of Science and Technology (grant number SAF2009-06954)

Appendix A. Supplementary data

Supplementary data related to this article can be found at http://dx.doi.org/10.1016/j.jaut.2012.12.005.

References

[1] Lefevre S, Knedla A, Tennie C, Kampmann A, Wunrau C, Dinser R, et al. Synovial fibroblasts spread rheumatoid arthritis to unaffected joints. Nat Med 2009;15:1414–20.
[2] Tolboom TC, van der Helm-Van Mil AH, Nelissen RG, Breedveld FC, Toes RE, Huizinga TW. Invasiveness of fibroblast-like synoviocytes is an individual patient characteristic associated with the rate of joint destruction in patients with rheumatoid arthritis. Arthritis Rheum 2005;52:1999–2002.
[3] Deaton AM, Bird A. CpG islands and the regulation of transcription. Genes Dev 2011;25:1010–22.
[4] Ball MP, Li JB, Gao Y, Lee JH, LeProust EM, Park IH, et al. Targeted and genome-scale strategies reveal gene-body methylation signatures in human cells. Nat Biotechnol 2009;27:361–8.
[5] Rauch TA, Wu X, Zhong X, Riggs AD, Pfeifer GP. A human B cell methylome at 100-base pair resolution. Proc Natl Acad Sci U S A 2009;106:671–8.
[6] Tili E, Michaille JJ, Costinean S, Croce CM. MicroRNAs, the immune system and rheumatic disease. Nat Clin Pract Rheumatol 2008;4:534–41.
[7] Selmi C, Lu Q, Humble MC. Heritability versus the role of the environment in autoimmunity. J Autoimmun 2012;39:249–52.
[8] Ballestar E. Epigenetics lessons from twins: prospects for autoimmune disease. Clin Rev Allergy Immunol 2010;39:30–41.
[9] Miller FW, Pollard KM, Parks CG, Germolec DR, Leung PS, Selmi C, et al. Criteria for environmentally associated autoimmune diseases. J Autoimmun 2012;39:253–8.
[10] Miller FW, Alfredsson L, Costenbader KH, Kamen DL, Nelson LM, Norris JM, et al. Epidemiology of environmental exposures and human autoimmune diseases: findings from a National Institute of Environmental Health Sciences Expert Panel Workshop. J Autoimmun 2012;39:259–71.
[11] Selmi C, Leung PS, Sherr DH, Diaz M, Nyland JF, Monestier M, et al. Mechanisms of environmental influence on human autoimmunity: a national institute of environmental health sciences expert panel workshop. J Autoimmun 2012;39:272–84.
[12] Germolec D, Kono DH, Pfau JC, Pollard KM. Animal models used to examine the role of the environment in the development of autoimmune disease: findings from an NIEHS Expert Panel Workshop. J Autoimmun 2012;39:285–93.
[13] Neidhart M, Rethage J, Kuchen S, Kunzler P, Crowl RM, Billingham ME, et al. Retrotransposable L1 elements expressed in rheumatoid arthritis synovial tissue: association with genomic DNA hypomethylation and influence on gene expression. Arthritis Rheum 2000;43:2634–47.
[14] Nile CJ, Read RC, Akil M, Duff GW, Wilson AG. Methylation status of a single CpG site in the IL6 promoter is related to IL6 messenger RNA levels and rheumatoid arthritis. Arthritis Rheum 2008;58:2686–93.
[15] Karouzakis E, Rengel Y, Jungel A, Kolling C, Gay RE, Michel BA, et al. DNA methylation regulates the expression of CXCL12 in rheumatoid arthritis synovial fibroblasts. Genes Immun 2011;12:643–52.
[16] Takami N, Osawa K, Miura Y, Komai K, Taniguchi M, Shiraishi M, et al. Hypermethylated promoter region of DR3, the death receptor 3 gene, in rheumatoid arthritis synovial cells. Arthritis Rheum 2006;54:779–87.
[17] Nakano K, Whitaker JW, Boyle DL, Wang W, Firestein GS. DNA methylome signature in rheumatoid arthritis. Ann Rheum Dis 2012.
[18] Niederer F, Trenkmann M, Ospelt C, Karouzakis E, Neidhart M, Stanczyk J, et al. Down-regulation of microRNA-34a* in rheumatoid arthritis synovial fibroblasts promotes apoptosis resistance. Arthritis Rheum 2012;64:1771–9.
[19] Nakamachi Y, Kawano S, Takenokuchi M, Nishimura K, Sakai Y, Chin T, et al. MicroRNA-124a is a key regulator of proliferation and monocyte chemoattractant protein 1 secretion in fibroblast-like synoviocytes from patients with rheumatoid arthritis. Arthritis Rheum 2009;60:1294–304.
[20] Stanczyk J, Ospelt C, Karouzakis E, Filer A, Raza K, Kolling C, et al. Altered expression of microRNA-203 in rheumatoid arthritis synovial fibroblasts and its role in fibroblast activation. Arthritis Rheum 2011;63:373–81.
[21] Bibikova M, Lin Z, Zhou L, Chudin E, Garcia EW, Wu B, et al. High-throughput DNA methylation profiling using universal bead arrays. Genome Res 2006;16:383–93.
[22] Dessau RB, Pipper CB. "R"–project for statistical computing. Ugeskr Laeger 2008;170:328–30.
[23] Du P, Kibbe WA, Lin SM. Lumi: a pipeline for processing illumina microarray. Bioinformatics 2008;24:1547–8.
[24] Gentleman RC, Carey VJ, Bates DM, Bolstad B, Dettling M, Dudoit S, et al. Bioconductor: open software development for computational biology and bioinformatics. Genome Biol 2004;5:R80.
[25] Falcon S, Gentleman R. Using GOstats to test gene lists for GO term association. Bioinformatics 2007;23:257–8.
[26] Smyth GK. Limma: linear models for microarray data. In: Bioinformatics and computational biology solutions using R and bioconductor; 2005. p. 397–420.
[27] Maksimovic J, Gordon L, Oshlack A. SWAN: subset-quantile within array normalization for illumina infinium HumanMethylation450 BeadChips. Genome Biol 2012;13:R44.
[28] Touleimat N, Tost J. Complete pipeline for infinium((R)) Human Methylation 450K BeadChip data processing using subset quantile normalization for accurate DNA methylation estimation. Epigenomics 2012;4:325–41.
[29] Aryee MJ, Wu Z, Ladd-Acosta C, Herb B, Feinberg AP, Yegnasubramanian S, et al. Accurate genome-scale percentage DNA methylation estimates from microarray data. Biostatistics 2011;12:197–210.
[30] Herman JG, Graff JR, Myohanen S, Nelkin BD, Baylin SB. Methylation-specific PCR: a novel PCR assay for methylation status of CpG islands. Proc Natl Acad Sci U S A 1996;93:9821–6.
[31] Del Rey MJ, Usategui A, Izquierdo E, Canete JD, Blanco FJ, Criado G, et al. Transcriptome analysis reveals specific changes in osteoarthritis synovial fibroblasts. Ann Rheum Dis 2012;71:275–80.
[32] Lewis BP, Burge CB, Bartel DP. Conserved seed pairing, often flanked by adenosines, indicates that thousands of human genes are microRNA targets. Cell 2005;120:15–20.
[33] Krek A, Grun D, Poy MN, Wolf R, Rosenberg L, Epstein EJ, et al. Combinatorial microRNA target predictions. Nat Genet 2005;37:495–500.
[34] Kertesz M, Iovino N, Unnerstall U, Gaul U, Segal E. The role of site accessibility in microRNA target recognition. Nat Genet 2007;39:1278–84.
[35] Griffiths-Jones S, Grocock RJ, van Dongen S, Bateman A, Enright AJ. miRBase: microRNA sequences, targets and gene nomenclature. Nucleic Acids Res 2006;34:D140–4.
[36] Betel D, Wilson M, Gabow A, Marks DS, Sander C. The microRNA.org resource: targets and expression. Nucleic Acids Res 2008;36:D149–53.
[37] Wang X, El Naqa IM. Prediction of both conserved and nonconserved microRNA targets in animals. Bioinformatics 2008;24:325–32.
[38] Vergoulis T, Vlachos IS, Alexiou P, Georgakilas G, Maragkakis M, Reczko M, et al. TarBase 6.0: capturing the exponential growth of miRNA targets with experimental support. Nucleic Acids Res 2011;40:D222–9.
[39] Xiao F, Zuo Z, Cai G, Kang S, Gao X, Li T. miRecords: an integrated resource for microRNA-target interactions. Nucleic Acids Res 2009;37:D105–10.
[40] Yang JH, Li JH, Shao P, Zhou H, Chen YQ, Qu LH. starBase: a database for exploring microRNA-mRNA interaction maps from Argonaute CLIP-Seq and Degradome-Seq data. Nucleic Acids Res 2011;39:D202–9.
[41] Kozomara A, Griffiths-Jones S. miRBase: integrating microRNA annotation and deep-sequencing data. Nucleic Acids Res 2011;39:D152–7.
[42] Al-Shahrour F, Diaz-Uriarte R, Dopazo J. FatiGO: a web tool for finding significant associations of Gene Ontology terms with groups of genes. Bioinformatics 2004;20:578–80.

[43] Sturn A, Quackenbush J, Trajanoski Z. Genesis: cluster analysis of microarray data. Bioinformatics 2002;18:207–8.
[44] Thompson CA. FDA approves tocilizumab to treat rheumatoid arthritis. Am J Health Syst Pharm 2010;67:254.
[45] Sun H, Gong S, Carmody RJ, Hilliard A, Li L, Sun J, et al. TIPE2, a negative regulator of innate and adaptive immunity that maintains immune homeostasis. Cell 2008;133:415–26.
[46] Swan C, Duroudier NP, Campbell E, Zaitoun A, Hastings M, Dukes GE, et al. Identifying and testing candidate genetic polymorphisms in the irritable bowel syndrome (IBS): association with TNFSF15 and TNFalpha. Gut 2012.
[47] Yazbeck R, Howarth GS, Abbott CA. Dipeptidyl peptidase inhibitors, an emerging drug class for inflammatory disease? Trends Pharmacol Sci 2009; 30:600–7.
[48] Ruth JH, Shahrara S, Park CC, Morel JC, Kumar P, Qin S, et al. Role of macrophage inflammatory protein-3alpha and its ligand CCR6 in rheumatoid arthritis. Lab Invest 2003;83:579–88.
[49] Waldburger JM, Palmer G, Seemayer C, Lamacchia C, Finckh A, Christofilopoulos P, et al. Autoimmunity and inflammation are independent of class II transactivator type PIV-dependent class II major histocompatibility complex expression in peripheral tissues during collagen-induced arthritis. Arthritis Rheum 2011;63:3354–63.
[50] Li G, Zhang Y, Qian Y, Zhang H, Guo S, Sunagawa M, et al. Interleukin-17A promotes rheumatoid arthritis synoviocytes migration and invasion under hypoxia by increasing MMP2 and MMP9 expression through NF-kappaB/HIF-1alpha pathway. Mol Immunol 2012;53:227–36.
[51] Solau-Gervais E, Zerimech F, Lemaire R, Fontaine C, Huet G, Flipo RM. Cysteine and serine proteases of synovial tissue in rheumatoid arthritis and osteoarthritis. Scand J Rheumatol 2007;36:373–7.
[52] Kawano S, Nakamachi Y. miR-124a as a key regulator of proliferation and MCP-1 secretion in synoviocytes from patients with rheumatoid arthritis. Ann Rheum Dis 2011;70(Suppl. 1):i88–91.
[53] He L, Hannon GJ. MicroRNAs: small RNAs with a big role in gene regulation. Nat Rev Genet 2004;5:522–31.
[54] Ngalamika O, Zhang Y, Yin H, Zhao M, Gershwin ME, Lu Q. Epigenetics, autoimmunity and hematologic malignancies: a comprehensive review. J Autoimmun 2012;39:451–65.
[55] Nakasa T, Miyaki S, Okubo A, Hashimoto M, Nishida K, Ochi M, et al. Expression of microRNA-146 in rheumatoid arthritis synovial tissue. Arthritis Rheum 2008;58:1284–92.
[56] Kobayashi K, Yagasaki M, Harada N, Chichibu K, Hibi T, Yoshida T, et al. Detection of Fcgamma binding protein antigen in human sera and its relation with autoimmune diseases. Immunol Lett 2001;79:229–35.
[57] Nishimoto N, Kishimoto T, Yoshizaki K. Anti-interleukin 6 receptor antibody treatment in rheumatic disease. Ann Rheum Dis 2000;59(Suppl. 1):i21–7.
[58] Watanabe Y, Takeuchi K, Higa Onaga S, Sato M, Tsujita M, Abe M, et al. Chondroitin sulfate N-acetylgalactosaminyltransferase-1 is required for normal cartilage development. Biochem J 2010;432:47–55.
[59] Sato T, Kudo T, Ikehara Y, Ogawa H, Hirano T, Kiyohara K, et al. Chondroitin sulfate N-acetylgalactosaminyltransferase 1 is necessary for normal endochondral ossification and aggrecan metabolism. J Biol Chem 2011;286: 5803–12.
[60] Leng L, Metz CN, Fang Y, Xu J, Donnelly S, Baugh J, et al. MIF signal transduction initiated by binding to CD74. J Exp Med 2003;197:1467–76.
[61] Simhadri VL, Hansen HP, Simhadri VR, Reiners KS, Bessler M, Engert A, et al. A novel role for reciprocal CD30-CD30L signaling in the cross-talk between natural killer and dendritic cells. Biol Chem 2012;393:101–6.
[62] Matsui T, Akahoshi T, Namai R, Hashimoto A, Kurihara Y, Rana M, et al. Selective recruitment of CCR6-expressing cells by increased production of MIP-3 alpha in rheumatoid arthritis. Clin Exp Immunol 2001;125:155–61.
[63] Ospelt C, Mertens JC, Jungel A, Brentano F, Maciejewska-Rodriguez H, Huber LC, et al. Inhibition of fibroblast activation protein and dipeptidylpeptidase 4 increases cartilage invasion by rheumatoid arthritis synovial fibroblasts. Arthritis Rheum 2010;62:1224–35.
[64] Buhligen J, Himmel M, Gebhardt C, Simon JC, Ziegler W, Averbeck M. Lysophosphatidylcholine-mediated functional inactivation of syndecan-4 results in decreased adhesion and motility of dendritic cells. J Cell Physiol 2010;225: 905–14.
[65] Nishimura WE, Costallat LT, Fernandes SR, Conde RA, Bertolo MB. Association of HLA-DRB5*01 with protection against cutaneous manifestations of rheumatoid vasculitis in Brazilian patients. Rev Bras Rheumatol 2012;52:366–74.
[66] Griffiths RJ, Smith MA, Roach ML, Stock JL, Stam EJ, Milici AJ, et al. Collagen-induced arthritis is reduced in 5-lipoxygenase-activating protein-deficient mice. J Exp Med 1997;185:1123–9.
[67] Manzo A, Vitolo B, Humby F, Caporali R, Jarrossay D, Dell'accio F, et al. Mature antigen-experienced T helper cells synthesize and secrete the B cell chemoattractant CXCL13 in the inflammatory environment of the rheumatoid joint. Arthritis Rheum 2008;58:3377–87.
[68] Pradhan D, Morrow J. The spectrin-ankyrin skeleton controls CD45 surface display and interleukin-2 production. Immunity 2002;17:303–15.